Open Access

Journal of Energy and Power Technology

Original Research

New Electrocatalysts Prepared by Co-Sputter Deposition for the Direct Oxidation of Methanol

Dan Fang ‡, Sri Narayan *

Department of Chemistry, University of Southern California, University Park, Los Angeles, California, USA; E-Mails: danfang@usc.edu; sri.narayan@usc.edu

‡ Current Affiliation: Carbon Capture, 130 W Union St, Pasadena, California, USA; E-Mail: dan@carboncapture.com

* **Correspondence:** Sri Narayan; E-Mail: sri.narayan@usc.edu

Academic Editor: Maria Helena de Sá

Special Issue: Design and Characterization of New Electrocatalysts for Low Temperature Fuel Cells

Journal of Energy and Power Technology
2021, volume 3, issue 3
doi:10.21926/jept.2103038

Received: May 25, 2021
Accepted: August 09, 2021
Published: August 13, 2021

Abstract

Direct methanol oxidation catalysts Pt_{1-x}-Ta_x (0<x<1) were prepared using co-sputter deposition. Characterization of these thin film catalysts was performed using scanning electron microscopy (SEM), energy dispersive X-ray (EDX), X-ray Diffraction (XRD) and X-ray photoelectron spectroscopy (XPS). Assessment of the methanol oxidation activity of Pt_{1-x}-Ta_x catalysts were achieved through half-cell experiments. Among all the Pt_{1-x}-Ta_x catalysts, $Pt_{0.77}$-$Ta_{0.23}$ catalyst showed the best electrochemical area specific activity which was comparable to platinum-ruthenium alloy on carbon (PtRu/C) catalysts. Pt_{1-x}-Ta_x catalysts worked as bi-functional methanol oxidation catalysts. The surface oxides species activated water molecules and hence facilitated the process of removing carbon monoxide from the platinum sites. The membrane electrode assembly (MEA) of $Pt_{0.77}$-$Ta_{0.23}$ catalyst was tested at 60, 80 and 90 °C. The power density achieved at 90 °C was 82 mW/cm^2/mg Pt, which was 1.82 times of PtRu/C catalyst with similar platinum loading.

Keywords
Electrocatalyst; methanol fuel cell; sputter deposition

1. Introduction

Direct methanol fuel cells (DMFCs) are attractive because of the high energy density of methanol [1], the overall simplicity of the fuel cell system [2, 3] and the ease of re-fueling with a liquid fuel. State-of-art DMFC systems use platinum-ruthenium catalysts at the anode, platinum catalysts at the cathode, with a proton-conducting polymer electrolyte membrane separating the two electrodes [4-6]. Thus far, the best commercial anode catalyst is a highly-dispersed platinum-ruthenium alloy (atomic ratio of Pt:Ru of 1:1) supported on high surface area carbon such as Vulcan XC-72. This catalyst is commercially available with 10wt.% to 80wt.% total metal loading. In this type of catalyst, the roles of platinum and ruthenium are quite distinct and hence it is referred to as a bi-functional catalyst [7]. Platinum dissociates the methanol molecule, while ruthenium dissociates the water molecule. The resulting adsorbed species, -CO_{ads} and -OH_{ads}, react on the surface to form carbon dioxide. The chemical equations below represent the process that occurs on the catalyst [8]:

$$\text{Methanol Dissociation: } Pt + CH_3OH \rightarrow Pt - H_{ads} + Pt{-}CO_{ads} \quad [1]$$

$$\text{Water Dissociation: } Ru + H_2O \rightarrow Ru - H_{ads} + Ru{-}OH_{ads} \quad [2]$$

$$\text{Surface Recombination: } Pt - CO_{ads} + Ru - OH_{ads} \rightarrow Pt + Ru + CO_2 + H^+ + e^- \quad [3]$$

Although this type of nano-particulate Pt-Ru catalyst is thus far the most active for the electro-oxidation of methanol [9], a large precious metal loading is required to realize practically relevant current densities. Approximately 60-80 grams of Pt-Ru alloy is required for a 1kW fuel cell. Additionally, the ruthenium part of the Pt-Ru catalyst is prone to oxidation and dissolution if certain threshold potentials are exceeded, limiting the durability of the catalyst. The accelerated degradation of ruthenium within six months of operation was observed in a 400-Watt, 80-cell direct methanol fuel cell stack by Valdez et al. [10, 11]. Thus, due to the high precious metal catalyst loadings and the relatively poor durability of ruthenium-based catalysts, the wide-spread commercialization of the direct methanol fuel cell to sizes larger than 1kW has not occurred.

Earlier research has indicated that tantalum and niobium are potential alternatives to ruthenium in methanol oxidation catalysts [12-14]. In these studies, it was shown that oxygen vacancies on the passivation layer of tantalum and niobium oxides activated water and therefore played the role of ruthenium in bi-functional catalysts. A tantalum-modified platinum electrode was studied and the bi-functional mechanism on tantalum-modified platinum was proposed by Masud et al. [13]. In another study, the methanol oxidation activity of Pt-Ta alloy showed improvement over a platinum catalyst [14]. Ta_2O_5-encapsulated platinum was prepared and showed improved methanol oxidation performance due to improved surface area [15]. Thus, the use of tantalum to replace ruthenium seemed promising to investigate. To this end, we examined Pt_{1-x}-Ta_x thin film catalysts produced by co-sputtering. The sputter-deposition method is well known for its potential in the synthesis of nanomaterials for electrochemical catalysts [16, 17]. It allowed us to prepare the catalyst with

platinum and tantalum in any desired ratio on a various of substrates. We have investigated the structure, morphology and composition of these catalysts by SEM, EDX and XPS. Quasi-steady state voltammetry tests of the catalysts suggested that the Pt_{1-x}-Ta_x catalysts acted through the bi-functional mechanism of methanol oxidation.

In some of the previous literature reports on $Pt_{1-x}Ta_x$ catalysts, a combinatorial approach was used with the focus on identifying the most active composition [14]. In our work, we have focused on understanding the effect of composition on the electrochemical parameters and demonstrating the benefits of these catalysts in practical methanol fuel cells. We have also tried to gain insight into the interaction between platinum and tantalum in enhancing the electro-oxidation of methanol that led to optimal catalytic activity, lowered the noble metal content, and enabled the use of these new catalysts in practical cells.

2. Materials and Methods

2.1 Materials Preparation

2.1.1 Preparation of Co-sputtered Pt_{1-x}-Ta_x Electrodes

Co-sputtered Pt_{1-x}-Ta_x electrodes were prepared in a custom-built multi-source sputter deposition system (Explorer Hybrid Coating System, Denton Vacuum). Each Pt_x-Ta_{1-x} electrode was generated by co-depositing platinum and tantalum onto a 2 cm by 2 cm carbon fiber composite paper substrate (AvCarb MGL 190). The main chamber was pumped down to 10^{-6} Torr before sputtering using a d.c. magnetron source. A five-minute pre-sputtering process was conducted to clean the target surface and remove any possible contamination. Then platinum (from a 2" target of purity 99.95%, Plasmaterials) and tantalum (from a 2" target of purity 99.95%, Plasmaterials) were co-deposited from separate d.c. magnetron sputter sources. The sputter power of the platinum cathode was held at 40 W while the sputter power of the tantalum cathode was varied between 20 to 140 W in steps of 20 W. The total catalyst amount was maintained the same while the platinum to tantalum ratio was varied. The background pressure during deposition was maintained at 10 mTorr by an argon flow rate of 35 sccm. The substrate holder was rotated at 20 rpm to ensure uniform lateral distribution of the metals in the films. The deposition rates were monitored with a quartz crystal monitor.

2.1.2 Membrane-Electrode Assemblies Preparation

The sputtered electrodes prepared in the manner described above were also tested in a full-cell configuration by fabricating membrane-electrode assemblies (MEAs). The MEA consisted of the sputtered electrode with the methanol oxidation catalyst as the anode, Nafion™ 117 as the polymer electrolyte membrane, and platinum black coated on a teflonized carbon fiber paper as the cathode. Specifically, co-sputtered $Pt_{0.77}$-$Ta_{0.23}$, prepared by co-sputtering Pt at 40W and Ta at 45 W at a background pressure of 30 mTorr, was selected for the full-cell experiments. The catalyst was sputtered onto a 5 cm by 5 cm carbon fiber composite paper (AvCarb MGL 190) coated with multi-walled carbon nanotubes (CNTs) in order to achieve a high electrode surface area for a certain geometric area of the carbon paper. The CNT was dispersed in water and spray coated on the carbon paper to achieve a loading of 0.01 mg/cm^2. The total catalyst loading of the anode was 0.15 mg/cm^2.

The platinum loading was 0.04 mg/cm^2. A thin coating of Nafion solution (Liquion 5% Nafion ionomer solution from Ion Power) was sprayed over the $Pt_{0.77}$-$Ta_{0.23}$ anode electrode to ensure a continuous proton-conducting path at the interface of the catalyst materials and Nafion membrane in the MEA. We used a hydrophobic substrate for the oxygen electrode and a hydrophilic (water wettable) substrate for the methanol oxidation electrode. Toray TGPH-060 was available readily with 20% Teflon and hence was used for the oxygen electrode. No comparable Toray product without Teflon was available. Consequently, for a Teflon-free substrate, the AvCarb MGL 190 material was used. Please note that besides their Teflon content, the two substrates were comparable in their properties (See supplementary material Figure S1 and Table S1).

A standard MEA was also fabricated with an anode consisting of commercial Pt-Ru/C catalyst coated on AvCarb MGL 190 carbon paper using catalyst inks prepared with Nafion solution (Liquion 5% Nafion), isopropanol and water. The mass ratio of PtRu catalyst to the Nafion solution was 1:5. The loading of platinum was 0.04 mg/cm^2, which was the same as the anode of the co-sputtered $Pt_{0.77}$-$Ta_{0.23}$ MEA. On the cathode side, the catalyst layers were coated on Toray carbon paper (TGPH-060, 20% teflonized) using inks containing platinum black and water. The platinum black loading of 2 mg/cm^2 on the cathode was maintained in all the full cell studies. The MEA was formed by hot-pressing the electrode-membrane sandwich at 140℃ under a load of about 440 kg for 15 minutes.

2.2 Materials Characterization

2.2.1 Physical Characterization

A JEOL JSM 7001 SEM was used to study the morphology of the sputtered catalysts. The metallic compositions of the catalysts were determined by EDX analysis using a Kevex Quantum Detector with an IXRF digital pulse processing analyzer microscope operated at 10 kV. The surface composition of the catalysts were investigated using XPS with a magnesium X-ray source (1253.6 eV, SPECS XPS at NETL). The XPS data was analyzed using CASA software and all the XPS data was corrected based on the carbon peak at 284.6 eV.

2.2.2 Half-Cell Electrochemical Measurement

Electrochemical studies at room temperature were carried out in the "half-cell" configuration using a three-electrode cell. A solution of 0.1 M perchloric acid was used as the electrolyte, a mercury/mercury sulfate (MSE) ($Hg|Hg_2SO_4$, 1M H_2SO_4, E^o = 0.650 V) electrode was used as the reference electrode, and a Pt wire was used as a counter electrode. A 2 x 2 cm^2 Toray paper coated electrode was used as the working electrode. Electrochemical studies were performed with a Potentiostat/Galvanostat/Frequency Response Analyzer (Ametek-PAR-VMC-4). In a typical measurement, the electrode potential was varied and the current response was measured. The solutions of 0.1 M perchloric acid were de-gassed to be free of oxygen by saturation with argon. A 1M solution of methanol in 0.1M perchloric acid was used in all the polarization studies. For the surface area studies, a 0.1 M perchloric acid solution free of methanol was used. The cyclic voltammetry scan between -0.6 V and 0 V vs MSE with a 200 mV/s scan rate yielded current peaks for the electro-sorption and desorption of hydrogen atoms. The charge under the electro-desorption peak for hydrogen atoms was used to calculate the electrochemically active surface area of the electrodes, after correcting for the double layer charging current. A charge density of 210

microcoulomb/cm^2 corresponding to a monolayer of adsorption of hydrogen atoms on the platinum sites was used in the surface area calculations [18].

2.2.3 Full-Cell Test

For the full cell tests, the MEA was assembled in fuel cell test hardware (Electrode area 25 cm^2, Electrochem Inc.). Silicone gaskets were used to achieve sealing. The anode was supplied with a 1M methanol flowing at 1.1 L/min. The total volume of solution in the reservoir was 2 liters. The cathode was fed with air flowing at 2 L/min at a pressure of 1.7 atm. The solution was circulated past the electrodes at 60 °C for 1 hour before the start of testing. Then, the cells were tested at 60 °C, 80 °C and 90 °C.

3. Results and Discussion

3.1 Physical Characterization of Co-Sputtered Platinum-Tantalum Catalysts

Platinum-Tantalum films prepared by co-sputter deposition on carbon fiber paper (AvCarbMGL 190) were studied by Scanning Electron Microscopy. The carbon-fiber paper substrate was a random arrangement of microfibers of about 10 microns in diameter (Figure 1a, b). There was no noticeable difference in the surface morphology of the bare carbon fiber paper and that coated with $Pt_{0.77}$-$Ta_{0.23}$ (Figure 1c, d) except for the slightly increased brightness caused by the back-scattering of electrons from the metal-covered surface. An SEM image of co-sputtered $Pt_{0.77}$-$Ta_{0.23}$ with higher resolution has been included in the supplemental materials (Figure S2). We have also included the SEM images of two of the tantalum-rich co-sputtered $Pt_{1-x}Ta_x$ with different platinum to tantalum ratios in the supplemental materials (Figure S3). The coverage by the Pt_xTa_{1-x} films was uniform and complete across the substrate. A glass slide that was placed by the side of the carbon fiber paper during co-sputter deposition, and the thickness of the resulting film was measured by profilometry. With the Ta-rich compositions, the image resolution was poor due to low electronic conductivity of the surface films leading to extensive charging of the sample. The elemental composition mapped using EDX (Figure S4) showed that the composition was uniform across the entire surface of the film. The atomic ratio and thickness of all the films of Pt_xTa_{1-x} prepared by sputter-deposition are shown in Table 1.

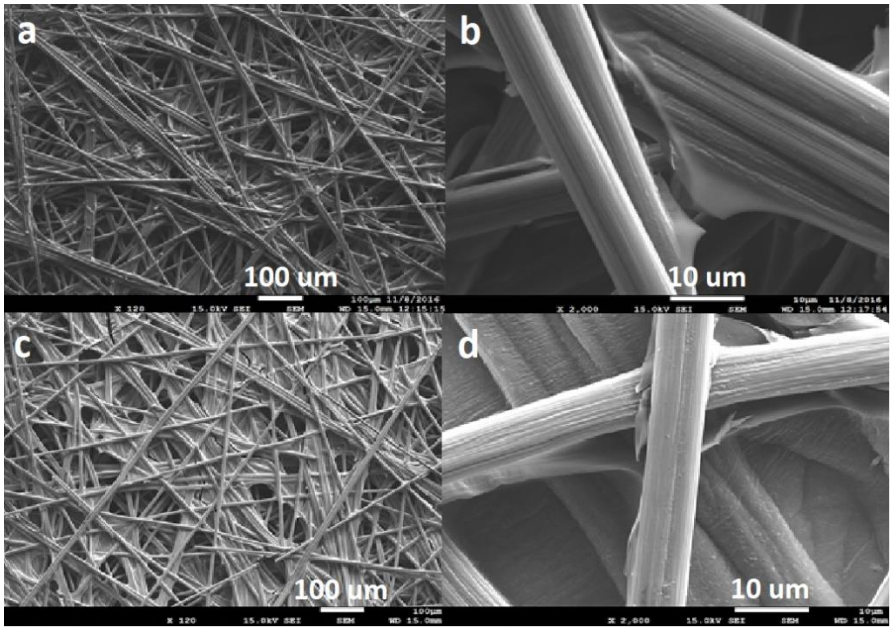

Figure 1 a and b: SEM images of Carbon-Fiber Paper (AvCarb MGL 190), c and d: Carbon-Fiber Paper co-sputtered with $Pt_{0.77}$-$Ta_{0.23}$.

Table 1 Composition and thickness of co-sputtered Pt_{1-x}-Ta_x films.

Tantalum Sputter Power/Watt	20	40	45	60	80	100	120	140
Platinum Sputter Power/Watt	40	40	40	40	40	40	40	40
Ta:Pt Atomic Ratio	0.132	0.264	0.298	0.957	1.34	1.55	1.69	1.83
Pt:Ta Stoichiometry	88:12	79:21	77:23	51:49	43:57	39:61	37:63	35:65
Ta_2O_5: Pt Volume Ratio	0.37	0.74	0.83	1.1	1.5	1.8	2.2	2.6
Catalyst Layer Thickness/nm	6.6	13	15	20	26	33	39	46

The XRD patterns of $Pt_{0.77}$-$Ta_{0.23}$ showed the face-centered cubic phase for platinum with prominent reflections from the (100) and (110) crystal faces, and orthorhombic tantalum(V) oxide, Ta_2O_5 (Figure 2). Absence of shift in the platinum peaks suggested that no solid solution was formed. The average crystallite size of platinum and tantalum oxide estimated using the Scherrer equation [19] to be 7.2 nm and 3.2 nm, respectively.

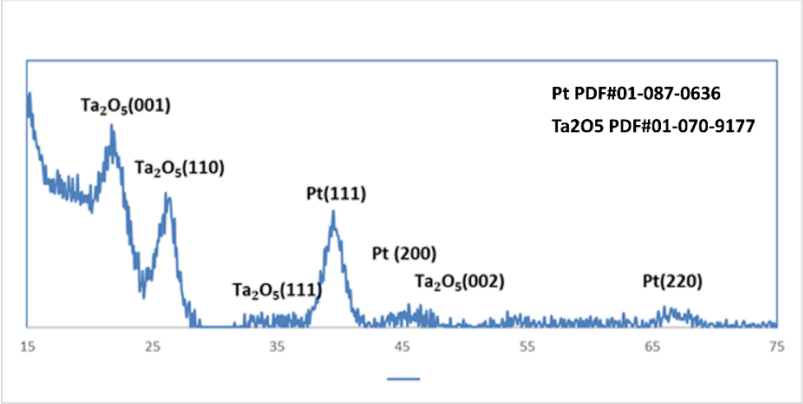

Figure 2 XRD patterns of the co-sputtered $Pt_{0.77}$-$Ta_{0.23}$ electrode.

XPS studies of the co-sputtered $Pt_{0.77}$-$Ta_{0.23}$ catalyst, confirmed the oxidation state of tantalum (V). However, in the $Pt_{0.77}$-$Ta_{0.23}$ catalyst, the binding energy of Ta-4f shifted to 25.75 eV compared to that of tantalum (V) oxide electrode prepared by sputter deposition, which was at 26.81 eV (Table S2 and Figure S5). On the other hand, the binding energy associated with the Pt-4f peak in co-sputtered $Pt_{0.77}$-$Ta_{0.23}$ was observed at 71.47 eV, exceeding slightly that of sputtered Pt which was 71.35 eV. These differences suggested a partial charge transfer from Pt to Ta in the sputtered films also reported in other studies [13, 14]. However, we noticed that the Ta 4f binding energy shifted to a greater extent than the Pt 4f binding energy. This shift could be attributed to the atomic ratio of Ta: Pt at 28.8%: 71.2%, whereupon for each tantalum atom there were three to four platinum atoms. Consequently, the effect of the interaction can be expected to be more pronounced on each of the tantalum atoms than on the Pt atoms.

In the electro-oxidation of methanol, the strong adsorption of CO on Pt poisons the active catalytic sites inhibiting the electro-oxidation reaction. This strong adsorption comes from two electron donation mechanisms. Firstly, donation from the σ bonding orbital of CO to the Pt 5d orbital and then next by back–donation of the Pt 5d orbital to the CO anti–bonding $2\pi^*_{CO}$ orbitals. When the d-electron density decreased via charge transfer to $TaO_{7/2}$, the Pt-CO binding energy can be expected to decrease. Thus, Ta can be expected to reduce the strength of adsorption of CO on platinum [20].

3.2 Half-Cell Electrochemical Characterizations of Co-Sputtered Platinum-Tantalum

The electrochemical characterization of the $Pt_{0.77}$-$Ta_{0.23}$ electrode was performed in a half-cell. The oxidation and reduction peaks in Figure 3 at -0.6 V vs MSE correspond to the electro-sorption and electro-desorption of hydrogen on the platinum sites. The amount of charge under the hydrogen desorption peak, was used to calculate the electrochemically-active surface area of the electrode. We found that the surface area of co-sputtered $Pt_{0.77}$-$Ta_{0.23}$ catalyst was 5 times that of the sputtered platinum catalyst of the same loading of platinum as $Pt_{0.77}$-$Ta_{0.23}$.

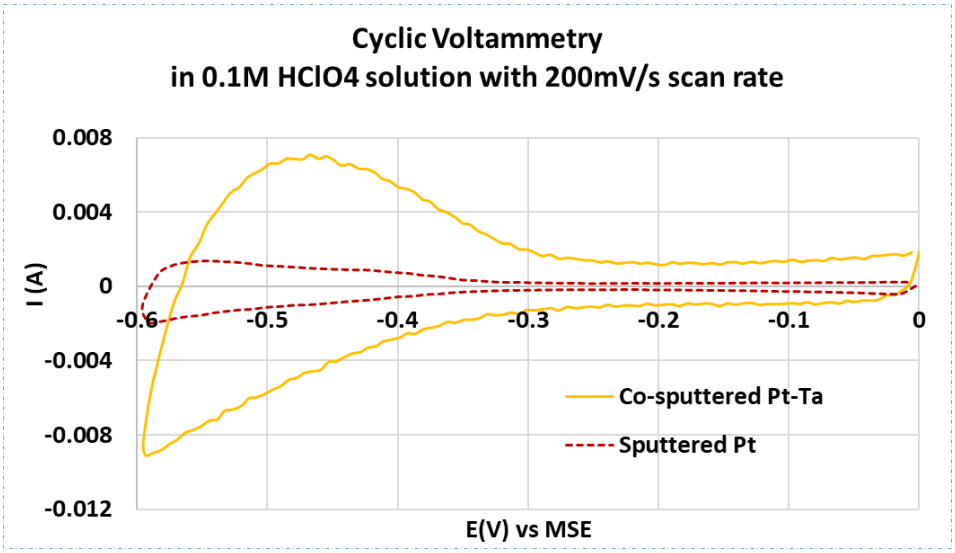

Figure 3 Cyclic voltammetric scans of co-sputtered $Pt_{0.77}$-$Ta_{0.23}$ and sputtered Pt at a scanning rate of 200 mV/s in 0.1 M perchloric acid.

This increase in surface area could not be attributed to the increased volume added by tantalum to the catalyst for the following reason. According to the platinum to tantalum atomic ratio from EDX elemental composition analysis, and the density of Pt and Ta_2O_5 being 21.45 g/cm^2 and 8.2 g/cm^2, respectively, the estimated volume ratio of Pt to Ta_2O_5 was 1:0.83. The total volume of co-sputtered $Pt_{0.77}$-$Ta_{0.23}$ could be expected to increase only about 1.83 times of the sputtered Pt sample with the same amount of Pt. The total platinum electrochemical surface area, however, was 5 times of sputtered Pt. We concluded that the morphology of Pt deposition had been changed by tantalum co-sputter deposition altering the growth of platinum deposits. To explain this observation, we proposed that in the sputtered platinum catalyst (Figure 4a), the platinum particles could grow on top of each of the other platinum particles whereas in the Pt_{1-x}-Ta_x structure (Figure 4b, c) with a moderate amount of tantalum, such growth was not possible allowing many more uncovered platinum sites to be present as shown in Figure 4d. The increased electrochemically active surface area of co-sputtered Pt_{1-x}-Ta_x catalyst was also an indication of a better utilization of platinum materials.

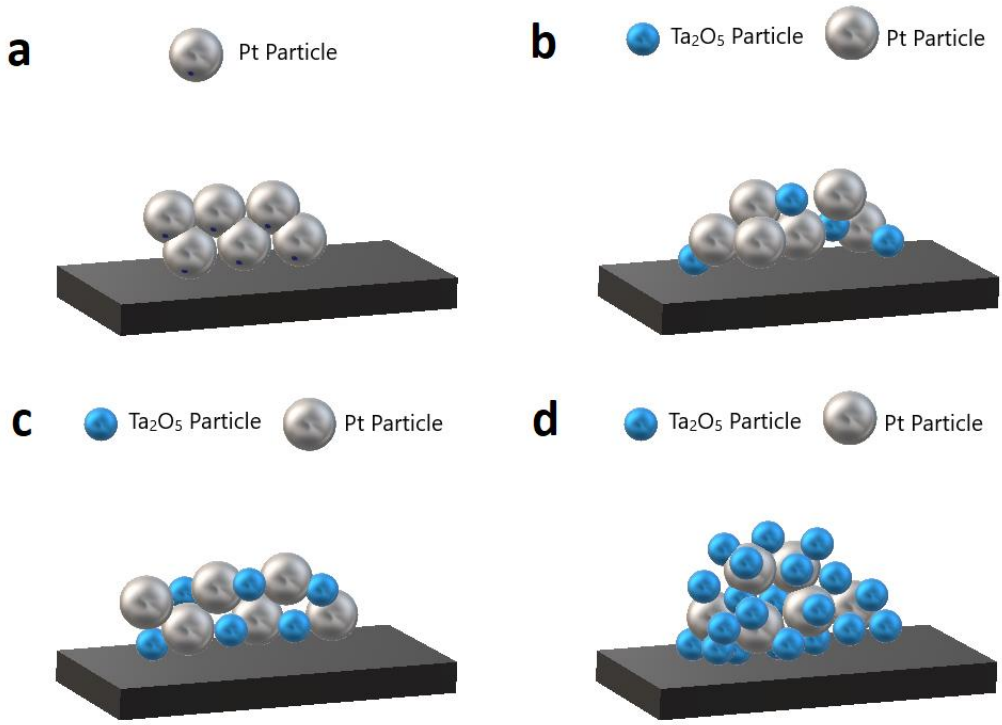

Figure 4 Illustrations of co-sputtered Pt_{1-x}-Ta_x ($0 \le x < 1$) catalysts with variant Ta to Pt atomic ratio (a) x = 0, (b) $0 < x < 0.23$, (c) x = 0.23 (b) $0.23 < x < 1$.

We also found that the electrochemically active surface area changed with the amount of Ta in the catalyst when the amount of platinum was maintained the same in all electrodes. The electrochemically active surface area (ECSA) and ECSA specific activity of co-sputtered Pt_{1-x}-Ta_x ($0 < x < 0.49$) was higher than for sputtered Pt catalyst (corresponding to x = 0). As shown in Figure 5, the electrochemically active surface area of platinum first increased with increasing amount of Ta and reached a maximum at Ta: Pt atomic ratio equals 0.364 and then started decreasing. The maximum platinum surface area on a 2 cm × 2 cm was 23.24 cm^2. The plausible architecture in the

film leading to the area increase is depicted in Figure 4. With increasing the amounts of Ta, the ECSA first increased because the Pt particles were better dispersed in the Pt_{1-x}-Ta_x catalyst (Figure 4b) compared to the aggregated Pt particles in Pt catalysts; at the maximum value of electrochemically active surface area (Figure 4c), tantalum particles helped platinum particles to disperse to the largest extent. In the meanwhile, all the platinum particles were still connected to the carbon substrate or other platinum particles. With further increase of Ta as in Figure 4d, some of the Pt particles could get isolated by the tantalum oxide particles. The poor electronic conductivity of the tantalum oxide could cause the decrease of access to the platinum particles and hence a decrease in the electrochemically active surface area of platinum.

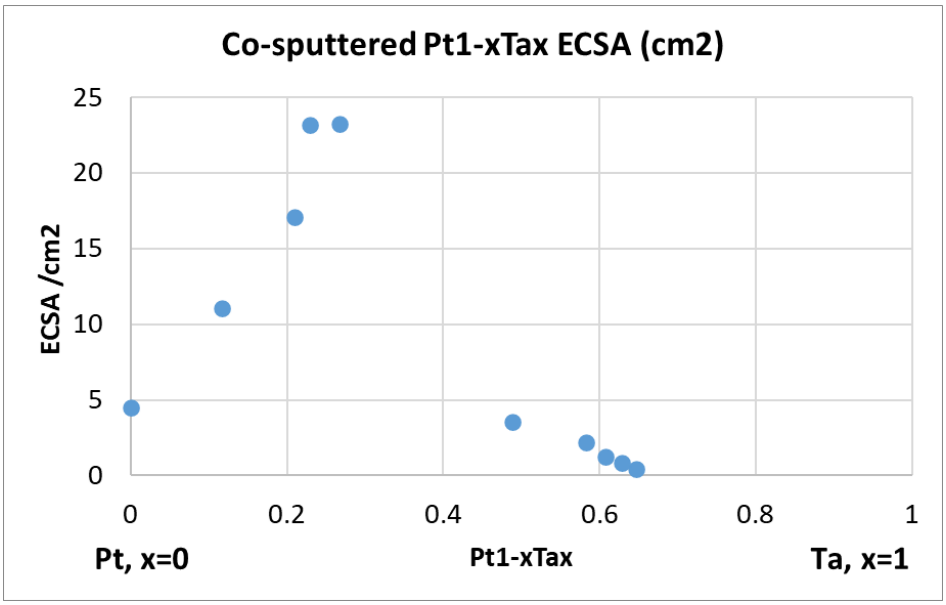

Figure 5 The effect of platinum to tantalum atomic ratio on the electrochemical surface area of co-sputtered Pt_{1-x}-Ta_x (0<x<1).

The electro-oxidation of methanol was studied at the sputter-deposited electrodes by slow-scan (quasi-steady-state) voltammetry and is shown in Figure 6. We compared the voltammetry of methanol oxidation for four different catalysts: co-sputtered $Pt_{0.77}$-$Ta_{0.23}$, co-sputtered Pt-Ru electrode with 1:1 atomic ratio, sputtered Pt and the commercial PtRu/C (commercial catalyst powder). The electrodes were anodically polarized in 1M solution of methanol in 0.1M perchloric acid over the potential range of -0.5 V to 0 V vs MSE at the slow scan rate of 1 mV/s. Onset potential of methanol oxidation in the anodic scan is a key metric for evaluating the catalyst activity [21]. We found that the commercial PtRu/C catalyst had a slightly higher onset potential compared with co-sputtered Pt-Ru catalyst, while both these values of onset potential were close to -0.3 V vs MSE. The onset potential of co-sputtered $Pt_{0.77}$-$Ta_{0.23}$ electrode was -0.15 V and that for the sputtered Pt was -0.125 V. The onset potential for the methanol oxidation reaction was indicative of the potential when the $-OH_{ads}$ coverage by water adsorption began to increase. Under these conditions, the adsorbed intermediate from water, namely, $-OH_{ads}$, could react with adsorbed $-CO_{ads}$ on the platinum sites leading to an oxidation current (Equation 3). These onset potential results were consistent with the water dissociation reaction that usually happens around -0.3 V vs MSE on ruthenium, -0.1 V on the platinum sites [22, 23]. Thus, based on the onset potential observed for

$Pt_{0.77}$-$Ta_{0.23}$, it was very likely that tantalum could dissociate water only at a potential equal or higher than -0.15 V vs. MSE.

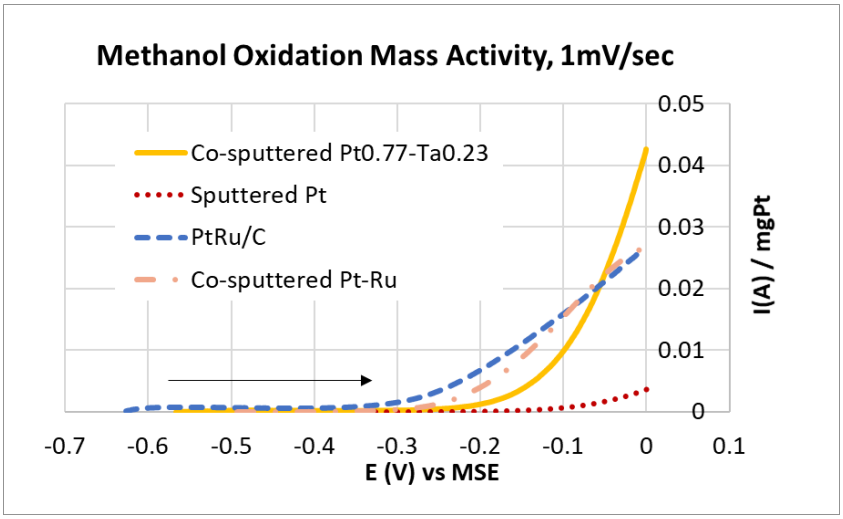

Figure 6 Pseudo-steady state methanol oxidation mass activities of co-sputtered $Pt_{0.77}$-$Ta_{0.23}$, co-sputtered Pt-Ru, sputtered Pt and PtRu/C in 0.1 M perchloric acid solution with 1M methanol.

The area specific activity for methanol oxidation is defined as the observed methanol oxidation current divided by the electrochemically active platinum surface area as determined from the hydrogen-desorption studies. In Figure 7, the area specific activity of the $Pt_{0.77}$-$Ta_{0.23}$ increased with the electrode potential at a greater rate than PtRu/C, and the activity exceeded PtRu/C at -0.12V vs MSE as we anodically polarized the electrode. The Pt electrode exhibited a low oxidation current as it was poisoned by the strong adsorption of CO adsorption on Pt sites. Upon reaching positive electrode potentials >0V vs. MSE, the water dissociation reaction was facilitated on the Pt sites and the adsorbed CO could be removed from the catalytic active surface to allow for further dissociation of methanol [24]. The methanol oxidation activities of co-sputtered $Pt_{0.77}$-$Ta_{0.23}$ catalyst at -0.1V and 0 V have been compared with PtRu/C and Pt in Table 2.

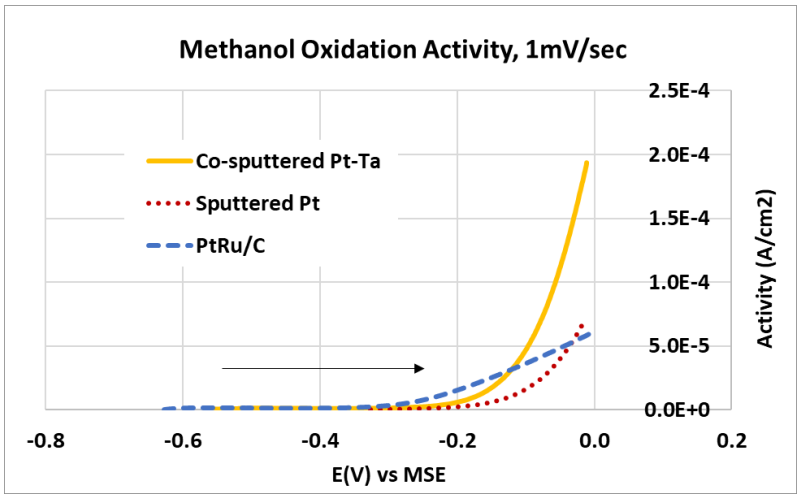

Figure 7 Pseudo-steady state methanol oxidation ECSA specific activities of co-sputtered $Pt_{0.77}$-$Ta_{0.23}$, sputtered Pt and PtRu/C in 0.1 M perchloric acid solution with 1M methanol.

Table 2 Co-sputtered $Pt_{0.77}$-$Ta_{0.23}$ catalyst ECSA specific activities compared to sputtered Pt and PtRu/C catalysts.

Potential	Co-sputtered Pt-Ta catalyst electrochemical area specific activity	
At-0.1V vs MSE	2.8 times of Pt	1.2 times of PtRu/C
At 0V vs MSE	2.3 times of Pt	3.2 times of PtRu/C

We also found that methanol oxidation activity of Pt_{1-x}-Ta_x catalyst was affected by the amount of Ta in the catalysts. In Figure 8, the activity first increased with increasing the amount of Ta. We attributed this to more and more platinum catalytic sites being in contact with tantalum sites so that more bi-functional catalytic sites were generated. $Pt_{0.77}$-$Ta_{0.23}$ had the highest activity. However, the activity decreased with further increase in tantalum content. We ascribed this to the Pt particles becoming isolated due to the higher content of tantalum oxide particles. Thus, the specific activity of co-sputtered Pt_{1-x}-Ta_x ($0<x<0.49$) was higher than sputtered Pt catalyst, corresponding to x = 0.

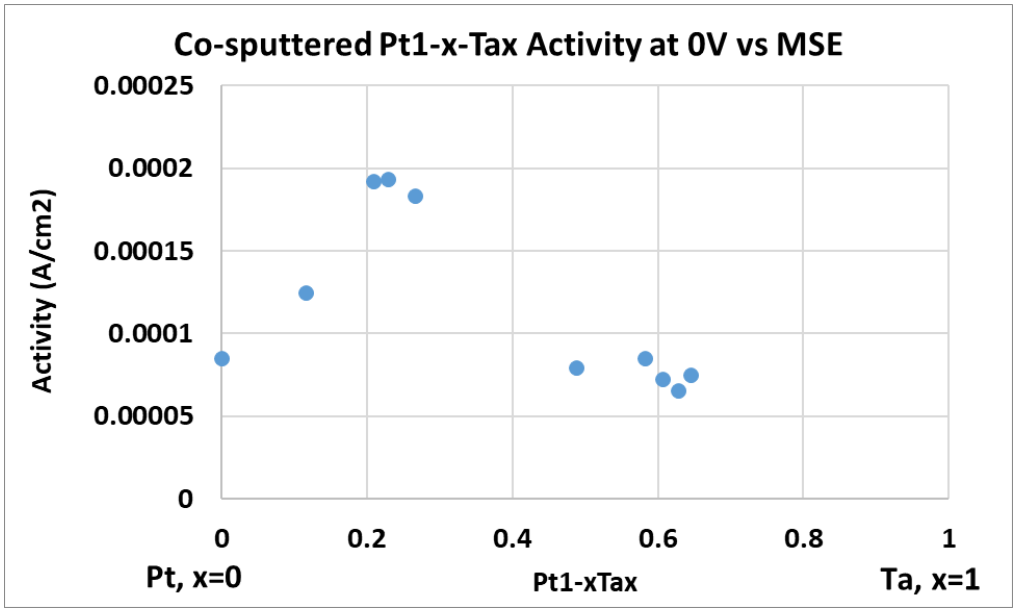

Figure 8 The effect of co-sputtered Pt_{1-x}-Ta_x catalysts composition on the methanol oxidation ECSA specific activity.

To test the stability of the electrocatalyst with the highest specific activity (the $Pt_{0.77}$-$Ta_{0.23}$ electrode), we carried out steady-state polarization tests at a relatively positive potential of -0.1V vs MSE as shown in Figure 9. The $Pt_{0.77}$-$Ta_{0.23}$ catalyst showed similar specific activity as the PtRu/C after holding at -0.1 V vs MSE for 1 hour. We attributed the gradual decrease and stabilization of the oxidation current on the co-sputtered $Pt_{0.77}$-$Ta_{0.23}$ to surface reconstruction. The similar sputtered electrodes including those with Pt-Ru also exhibited the same type of decrease before stabilization as shown in Figure S6. Upon stabilization the rate of change of current after 3600 seconds was 0.0029% per second for co-sputtered $Pt_{0.77}$-$Ta_{0.23}$ while that for the co-sputtered Pt-Ru catalyst was 0.0115% per second. These values suggested that at -0.1 V vs. MSE, $Pt_{0.77}$-$Ta_{0.23}$ catalyst resisted deactivation better than the co-sputtered Pt-Ru catalyst.

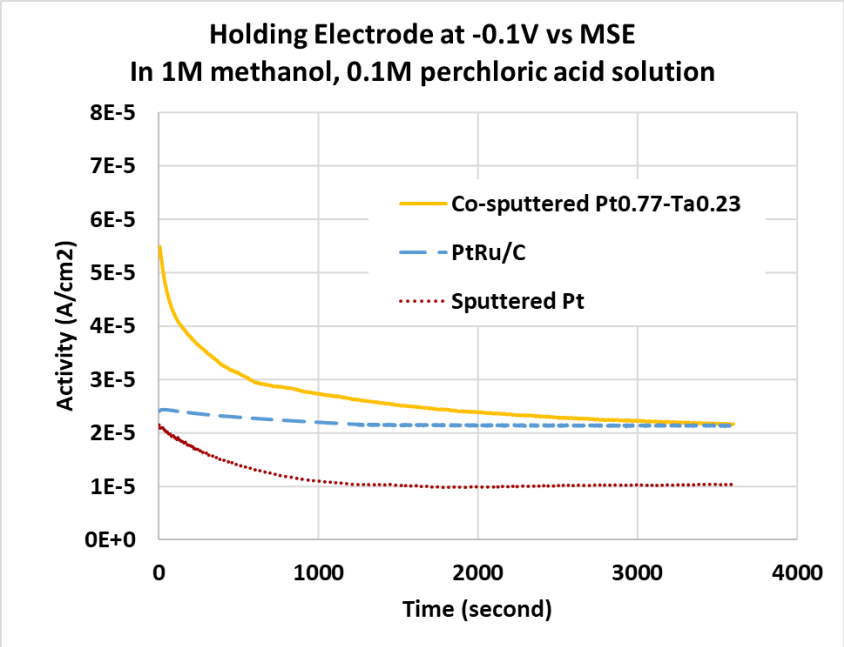

Figure 9 Electrode electrochemical stability test by holding co-sputtered $Pt_{0.77}$-$Ta_{0.23}$, PtRu/C and sputtered Pt electrodes at -0.1V vs MSE for 1 hour.

3.3 Methanol Oxidation Mechanism of Co-Sputtered Platinum-Tantalum Catalysts

Tafel slopes of co-sputtered $Pt_{0.77}$-$Ta_{0.23}$, sputtered-Pt and PtRu/C electrodes are compared in Figure 10 and Table 3. The Tafel slopes of co-sputtered $Pt_{0.77}$-$Ta_{0.23}$, Pt-Ru/C and sputtered Pt over the range of -0.3V<V< -0.15V vs MSE potential region were similar indicating similar kinetic behavior, with a rate-determining step corresponding to a one-electron transfer process [25]. The Tafel slope of PtRu/C in the range of -0.15V<V<0V vs MSE was higher than -0.3V to -0.15V, suggesting a change in the mechanism. Earlier research showed that the limiting currents of PtRu/C in this potential region are not mass-transfer controlled and cannot be enhanced by changing the rotating speed of the rotating disk electrode in a half-cell experiment [26].

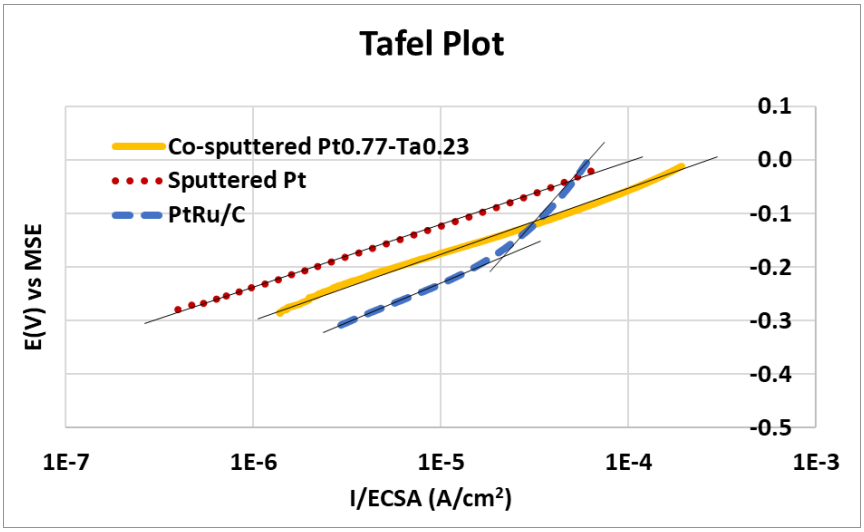

Figure 10 Methanol oxidation reaction Tafel plots of co-sputtered $Pt_{0.77}$-$Ta_{0.23}$, sputtered Pt and PtRu/C.

Table 3 Tafel slopes of Tafel plot of Co-sputtered $Pt_{0.77}$-$Ta_{0.23}$, Sputtered Pt and PtRu/C.

Electrode	Tafel slope	Potential Range
Co-sputtered $Pt_{0.77}$-$Ta_{0.23}$	119 mV/dec	-0.3V<V<0V
Sputtered Pt	117 mV/dec	-0.3V<V<0V
PtRu/C	143 mV/dec 376 mV/dec	-0.3V<V<-0.15V -0.15V<V<0V

We also found that changing the amount of tantalum in the catalyst affected the Tafel Slope for methanol oxidation as shown in Figure 11. The Tafel slope at low Ta percentage was 120 mV/dec, that suggested the rate-determining step to be a one-electron transfer step. As previously discussed, it was attributed to the surface recombination step. At higher values of Ta percentage, the Tafel slope first increased to 300mV/dec. The most likely rate-determining step at these potentials was the step of methanol dissociation. Further increase in the percentage of Ta resulted in a Tafel slope of about 500 mV. XRD studies on co-sputtered $Pt_{0.35}$-$Ta_{0.65}$ and $Pt_{0.43}$-$Ta_{0.57}$ electrodes suggested that for Ta content of >60% the surface was rich in Ta_2O_5 and TaO_2 as shown in Figure 12. The insulating property of these oxides would then explain the anomalously high Tafel slope.

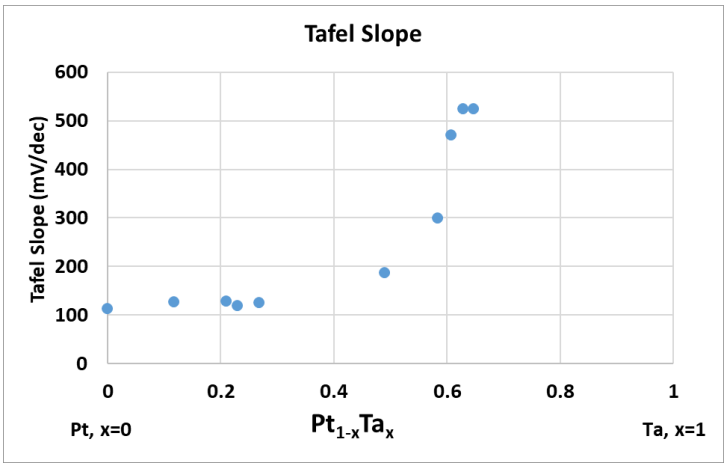

Figure 11 The effect of Pt_{1-x}-Ta_x catalysts composition on the methanol oxidation Tafel slope.

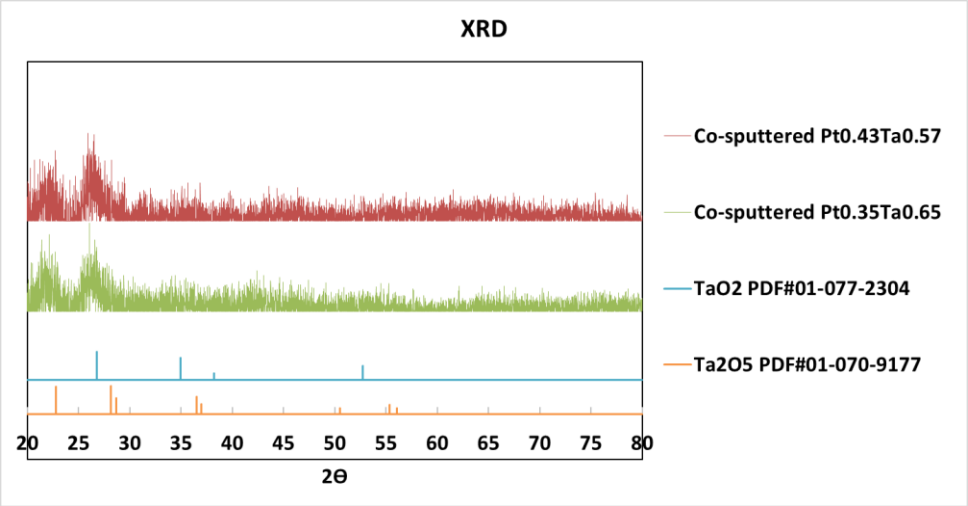

Figure 12 XRD pattens of co-sputtered $Pt_{0.35}$-$Ta_{0.65}$ and $Pt_{0.43}$-$Ta_{0.57}$ electrode.

As we discussed earlier, the specific activity of co-sputtered Pt_{1-x}-Ta_x (0<x<0.49) was higher than sputtered Pt. Further, the decrease in onset potential also suggested that Ta played an active role in enhancing the kinetics of the methanol oxidation reaction. Based on the metal oxides' ability to activate the water molecule and the Tafel Slope values, we propose the bi-functional mechanism on Pt_{1-x}-Ta_x catalysts shown schematically in Figure 13 and in equations 4-6. The rate determining step is the one-electron surface recombination step.

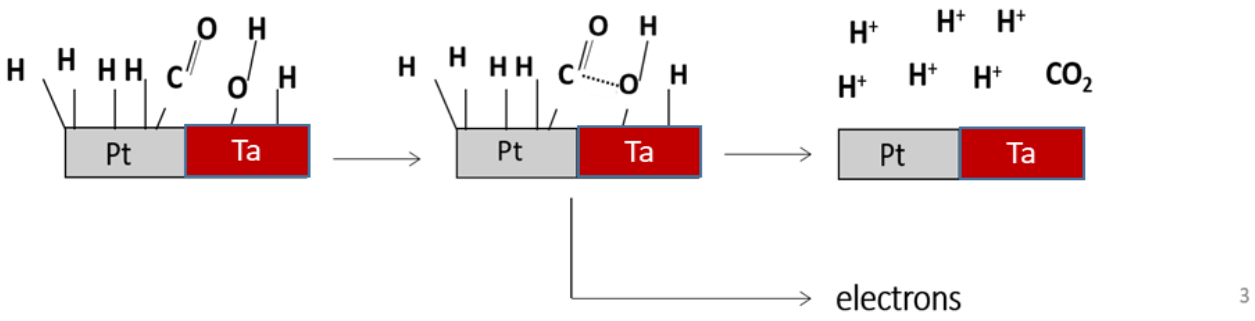

Figure 13 Co-sputtered Pt_{1-x}-Ta_x catalyst as a bi-functional catalyst for methanol oxidation.

$$\text{Methanol Dissociation: } Pt + CH_3OH \rightarrow Pt - H_{ads} + Pt{-}CO_{ads} \quad [4]$$

$$\text{Water Dissociation: } TaO_x + H_2O \rightarrow TaO_x - H_{ads} + TaO_x{-}OH_{ads} \quad [5]$$

$$\text{Surface Recombination: } Pt - CO_{ads} + TaO_x - OH_{ads} \rightarrow Pt + TaO_x + CO_2 + H^+ + e^- \quad [6]$$

3.4 Full-Cell Performance of the Membrane-Electrode Assemblies

Figure 14 shows the cell voltage and cell power density as a function of the current density for direct methanol fuel cells that use co-sputtered $Pt_{0.77}$-$Ta_{0.23}$ and PtRu/C as anode catalysts. The loading of platinum in PtRu/C electrode was 0.67 mg, and that of co-sputtered $Pt_{0.77}$-$Ta_{0.23}$ electrode

was 0.69 mg. The full cells with both these anode catalysts were studied at 90 °C, 80 °C and 60 °C in 1 M methanol with oxygen flowing through the positive electrode at 2 lpm and at 1.7 atm.

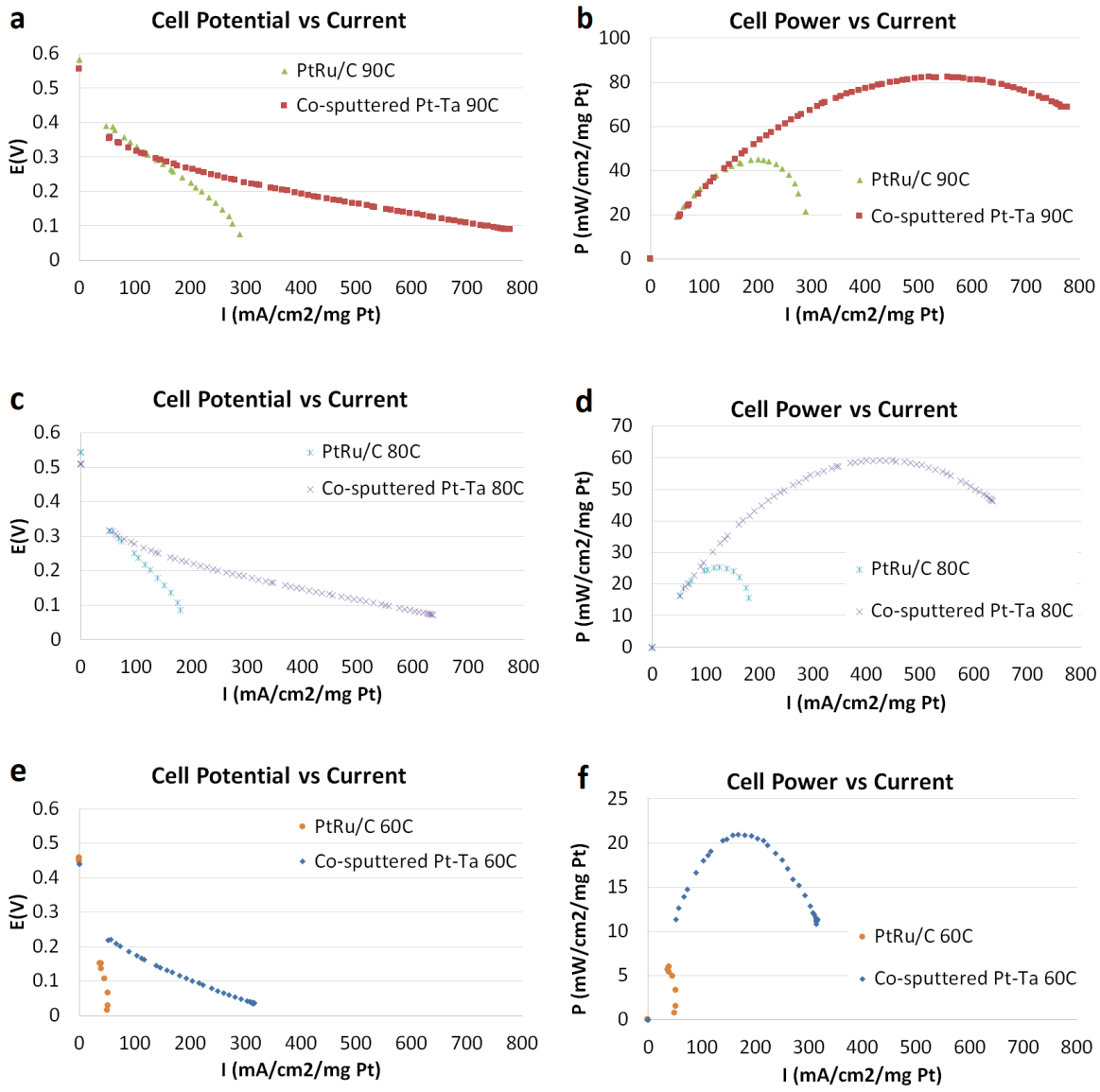

Figure 14 Cell voltage and cell power density of the direct methanol fuel cells with co-sputtered $Pt_{0.77}$-$Ta_{0.23}$ and PtRu/C as anode catalysts at 90 °C (a)(b), 80 °C (c)(d) and 60 °C (e)(f), in 1 M methanol with 2 Lpm oxygen at 1.7 atm.

The maximum power densities of the cells with $Pt_{0.77}$-$Ta_{0.23}$ were higher than that with PtRu/C at all the temperatures studied (Table 4). The best performance for both PtRu/C and $Pt_{0.77}$-$Ta_{0.23}$ were attained at 90 °C. Current densities as high as 300 mA/cm^2 could be supported on the Pt-Ta catalysts. At a cell voltage of 300 mV, the current normalized for platinum loading was 139 mA/(cm^2×mg$_{Pt}$) (at 95.6 mA/cm^2). The maximum power density was achieved by $Pt_{0.77}$-$Ta_{0.23}$ at 82 mA/(cm^2×mg$_{Pt}$) (57mW/cm^2 with a platinum loading of only 0.028 mg/cm^2), 1.82 times of that of a state-of-the-art PtRu/C catalyst. This result is comparable to the work of Witham et al, where the PtRu MEA made by sputter deposition showed a power density of 75 mW/cm^2 at a platinum loading of 0.02 mg/cm^2.[1]

The maximum current of $Pt_{0.77}$-$Ta_{0.23}$ was 778 mA/(cm^2-mg_{Pt}), 2.7 times that of PtRu/C. Although we did not collect any long-term durability data, we must note each run of our current-voltage tests was carried out over a 20 minutes period. During these tests, the electrodes experienced temperature in the range of 60-90 degrees Celsius and current densities in the range of 100-600 mA/cm^2. No noticeable performance change was noticed in these tests. These results suggested that the catalysts were durable at least in the short term.

Table 4 Maximum power densities and current densities of co-sputtered $Pt_{0.77}$-$Ta_{0.23}$ and PtRu/C.

MEAs		**90 °C**	**80 °C**	**60 °C**
Co-sputtered $Pt_{0.77}$-$Ta_{0.23}$	Maximum Power Density mW/cm^2/mg_{Pt}	82	59	21
	Maximum Current Density mA/cm^2/mg_{Pt}	778	635	314
PtRu/C	Maximum Power Density mW/cm^2/mg_{Pt}	45	25	6.0
	Maximum Current Density mA/cm^2/mg_{Pt}	289	180	50.1

4. Conclusion

In this paper, a series of thin film Pt_{1-x}-Ta_x catalysts were prepared by the sputter deposition method. The method can also be applied to any supporting electrode substrate. Such a method is also amenable for rapid throughput and scale-up as indicated by the work of 3M on sputter-deposited catalysts [27]. The $Pt_{0.77}$-$Ta_{0.23}$ catalyst showed similar specific activity (based on electrochemically active area) comparable to commercial-available PtRu/C catalysts. We found that the atomic ratio of platinum to tantalum in the catalyst affected the platinum-normalized methanol oxidation activity and suggested that in the Pt_{1-x}-Ta_x ($0<x<0.49$) catalysts the methanol oxidation reaction was activated by tantalum. The surface oxides of tantalum can activate water molecules and hence facilitate the process of removing carbon monoxide from platinum sites. Direct methanol fuel cells with $Pt_{0.77}$-$Ta_{0.23}$ catalyst achieved a platinum-normalized power density of 82 mW/(cm^2-mg_{Pt}) at 90 degrees Celsius which is 1.82 times of PtRu/C catalyst. As per our knowledge, this is the first time a tantalum-containing catalyst has been tested in a membrane-electrode assembly (MEA) for methanol oxidation. In the supplementary materials (Table S3) we provide a summary of the MEA performance of binary Pt-X catalysts synthesized by sputter-deposition and tested under comparable conditions in an effort to provide some benchmarking on the performance of the catalysts studied in this work. The scalability of sputter-deposition method and the lower noble metal content are beneficial for the practical use of these new catalysts.

Acknowledgments

The authors thank Dr A. Manivannan for his help with the XPS measurement. The authors thank Dr Bo Yang at University of Southern California for his assistance with setting up the testing systems.

The instrumentation support from the staff at Loker Hydrocarbon Institute at University of Southern California is acknowledged.

Additional Materials

The following additional materials are uploaded at the page of this paper.

1. Figure S1: SEM images of Toray paper TGPH-060 (Left) and AvCarb paper MGL 190 (Right).
2. Table S1: The properties of carbon fiber paper TGPH-060 and AvCarb MGL.
3. Figure S2: The highest resolution SEM image of co-sputtered $Pt_{0.77}$-$Ta_{0.23}$ electrode.
4. Figure S3: SEM image of co-sputtered $Pt_{0.43}$-$Ta_{0.57}$ electrode (Left) and co-sputtered $Pt_{0.37}$-$Ta_{0.63}$ electrode (Right).
5. Figure S4: EDX elemental mapping of (a) platinum and (b) tantalum.
6. Table S2: Binding energy of co-sputtered $Pt_{0.77}$-$Ta_{0.23}$, sputter Pt and sputter Ta.
7. Figure S5: Co-sputter Pt-Ta XPS spectra, (a) Ta-4f and (b) Pt-4f binding energy, XPS spectra were corrected using carbon spectra as a standard
8. Figure S6: Electrode electrochemical stability test by holding co-sputtered $Pt_{0.77}$-$Ta_{0.23}$, PtRu/C, Co-sputtered Pt-Ru and sputtered Pt electrodes at -0.1V vs MSE for one hour
9. Table S3: A summary of the methanol oxidation performance of MEAs with binary Pt-X catalyst synthesized by sputter deposition in current and previous research work.

Author Contributions

Dr Dan Fang performed the experiments and the analysis. Professor Sri R Narayan supervised her research.

Funding

This work was supported by Loker Hydrocarbon Institute at University of Southern California.

Competing Interests

The authors have declared that no competing interests exist.

References

1. Olah GA. The methanol economy. Chem Eng News. 2003; 81: 5.
2. Surampudi S, Narayanan SR, Vamos E, Frank H, Halpert G, LaConti AN, et al. Advances in direct oxidation methanol fuel cells. J Power Sources. 1994; 47: 377-385.
3. McGrath KM, Prakash GS, Olah GA. Direct methanol fuel cells. J Ind Eng Chem. 2004; 10: 1063-1080.
4. Prakash GKS, Olah GA, Smart MC, Narayanan SR, Wang QS, Surumpudi S, et al. Novel polymer electrolyte membranes for use in methanol fuel cells. Washington: US Patent; 1998; WO1998022989A1.
5. Prakash GS, Krause FC, Viva FA, Narayanan SR, Olah GA. Study of operating conditions and cell design on the performance of alkaline anion exchange membrane based direct methanol fuel

cells. J Power Sources. 2011; 196: 7967-7972.
6. Valdez TI, Narayanan SR. Effect of fabrication technique on direct methanol fuel cells designed to operate at low airflow. ECS Proc Volumes. 2002; 2002: 506.
7. Whitacre JF, Valdez T, Narayanan SR. Investigation of direct methanol fuel cell electrocatalysts using a robust combinatorial technique. J Electrochem Soc. 2005; 152: A1780-A1789.
8. Arico AS, Srinivasan S, Antonucci V. DMFCs: From fundamental aspects to technology development. Fuel Cells. 2001; 1: 133-161.
9. Moura AS, Fajín JL, Mandado M, Cordeiro MN. Ruthenium-platinum catalysts and direct methanol fuel cells (DMFC): A review of theoretical and experimental breakthroughs. Catalysts. 2017; 7: 47.
10. Piela P, Eickes C, Brosha E, Garzon F, Zelenay P. Ruthenium crossover in direct methanol fuel cell with Pt-Ru black anode. J Electrochem Soc. 2004; 151: A2053.
11. Valdez TI, Firdosy S, Koel B, Narayanan SR. Investigation of ruthenium dissolution in advanced membrane electrode assemblies for direct methanol based fuel cell stacks. ECS Trans. 2006; 1: 293-303.
12. Tague ME, Gregoire JM, Legard A, Smith E, Dale D, Hennig R, et al. High Throughput thin film Pt-M alloys for fuel electrooxidation: Low concentrations of M (M = Sn, Ta, W, Mo, Ru, Fe, In, Pd, Hf, Zn, Zr, Nb, Sc, Ni, Ti, V, Cr, Rh). J Electrochem Soc. 2012; 159: F880.
13. Masud J, Alam MT, Awaludin Z, El-Deab MS, Okajima T, Ohsaka T. Electrocatalytic oxidation of methanol at tantalum oxide-modified Pt electrodes. J Power Sources. 2012; 220: 399-404.
14. Gregoire JM, Tague ME, Cahen S, Khan S, Abruna HD, DiSalvo FJ, et al. Improved fuel cell oxidation catalysis in $Pt_{1-x}Ta_x$. Chem Mater. 2010; 22: 1080-1087.
15. Park KW, Sung YE. Pt nanostructured electrode encapsulated by a tantalum oxide for thin-film fuel cell. J Vac Sci Technol B Microelectron Nanom Struct. 2004; 22: 2628-2631.
16. Wang F, Zhao H, Liang J, Li T, Luo Y, Lu S, et al. Magnetron sputtering enabled synthesis of nanostructured materials for electrochemical energy storage. J Mater Chem A. 2020; 8: 20260-20285.
17. Liang J, Liu Q, Li T, Luo Y, Lu S, Shi X, et al. Magnetron sputtering enabled sustainable synthesis of nanomaterials for energy electrocatalysis. Green Chem. 2021; 23: 2834-2867.
18. Trasatti S, Petrii OA. Real surface area measurements in electrochemistry. Pure Appl Chem. 1991; 63: 711-734.
19. Patterson AL. The Scherrer formula for X-ray particle size determination. Phys Rev. 1939; 56: 978-982.
20. Blyholder G. Molecular orbital view of chemisorbed carbon monoxide. J Phys Chem C. 1964; 68: 2772-2777.
21. Geng D, Lu G. Dependence of onset potential for methanol electrocatalytic oxidation on steric location of active center in multicomponent electrocatalysts. J Phys Chem C. 2007; 111: 11897-11902.
22. Kakati N, Maiti J, Lee SH, Jee SH, Viswanathan B, Yoon YS. Anode catalysts for direct methanol fuel cells in acidic media: Do we have any alternative for Pt or Pt-Ru? Chem Rev. 2014; 114: 12397-12429.
23. Wasmus S, Küver A. Methanol oxidation and direct methanol fuel cells: A selective review. J Electroanal Chem. 1999; 461: 14-31.
24. Liu H, Zhang J. Electrocatalysis of direct methanol fuel cells: From fundamentals to applications.

Weinheim: Wiley-VCH Verlag GmbH & Co. KGaA; 2009.
25. Vidaković T, Christov M, Sundmacher K. Rate expression for electrochemical oxidation of methanol on a direct methanol fuel cell anode. J Electroanal Chem. 2005; 580: 105-121.
26. Li L, Xing Y. Methanol electro-oxidation on Pt-Ru alloy nanoparticles supported on carbon nanotubes. Energies. 2009; 2: 789-804.
27. Debe MK. Electrocatalyst approaches and challenges for automotive fuel cells. Nature. 2012; 486: 43-51.
28. Witham CK, Chun W, Valdez TI, Narayanan SR. Performance of direct methanol fuel cells with sputter-deposited anode catalyst layers. Electrochem Solid State Lett. 2000; 3: 497-500.
29. Caillard A, Coutanceau C, Brault P, Mathias J, Léger JM. Structure of Pt/C and PtRu/C catalytic layers prepared by plasma sputtering and electric performance in direct methanol fuel cells (DMFC). J Power Sources. 2006; 162: 66-73.
30. Jeong W, Cho GY, Cha SW, Park T. Surface roughening of electrolyte membrane for Pt-and Ru-sputtered passive direct methanol fuel cells. Materials. 2019; 12: 3969.
31. Nakashima T, Saito H, Murano K, Fukuhara C, Sudoh M. Design of multi-layer anode for direct methanol fuel cell. Electrochemistry. 2011; 79: 361-363.
32. Xinyao Y, Zhongqing J, Yuedong M. Preparation of anodes for DMFC by Co-sputtering of platinum and ruthenium. Plasma Sci Technol. 2010; 12: 224.
33. Park KW, Lee YW, Sung YE. Nanostructure catalysts prepared by multi-sputtering deposition process for enhanced methanol electrooxidation reaction. Appl Catal B. 2013; 132: 237-244.